Chapter 4

Literature survey: Polarimetric study of comets

In this Chapter, beginning era of polarimetric observations of comets has been cited first, followed by the modern era. After that, various features of cometary polarization, studied so far have been discussed. This includes phase angle, wavelength dependence of cometary polarization, modeling of phase curve, coma morphology, polarization map, simulation etc.

4.1 Partial linear polarization of comets

The solar light scattered by cometary atmosphere is partially elliptically polarized. The circular component is very small compared to linear one, and can be neglected. Thus, the light scattered by cometary atmosphere is considered as partially linearly polarized. The theory had been already discussed in chapter 2. For measurement purpose, working formula depending upon the polarimeter used in telescope at different observatories; had been already discussed for IUCAA Girawali Observatory (IGO) and Haute-Provence Observatory (OHP) in chapter 3).

The total intensity and the polarization degree are retrieved from measurements of the two polarized components of the brightness, respectively perpendicular and parallel to the scattering plane (I_l and I_r). Writing the formula for polarization in a generalised form-

$$I = I_l + I_r \tag{4.1a}$$

$$P = \frac{I_l + I_r}{I_l - I_r} \tag{4.1b}$$

The brightness variations with the distances to the Sun (R) and to the Earth (Δ) depend not only upon the distances but also upon changes in the activity of the comet and upon the size of the coma. Since the polarization is a ratio (remaining between 1 and +1), no normalization in brightness is required to compare data obtained on different objects (or on the same object at different times).

4.2 Polarimetric observations of comets: beginning to modern era

The polarimetric investigations of comets began with the discovery of traces of polarization in the light coming from the Great Comet 1819 II by François Arago. He also confirmed the non-zero polarization of light coming from comet Halley in 1835. ([Arago, 1854], [Arago, 1857])

The modern era of polarimetric studies of comets began with the work by Yngve Öhman ([Öhman, 1939], [Öhman, 1941]). He was the first to observe separately the polarization in the continuum and in emission bands. He explained for the first time that; the observed polarization (P_O) in cometary light is produced mainly due to two mechanisms: (i) Diffuse reflection, diffraction, scattering of light by dust particles in comet (P_C); (ii) Resonance Fluorescence emission of cometary molecules (P_E). Thus, P_O=P_C+P_E, provided these two quantities have the same direction vectors. Therefore, a study of the continuum alone gives information about the solid particles in the comet, and that of the emission lines gives information about the excitation and emission processes ([Öhman, 1941], [Blackwell and Willstrop, 1957], [Bastien et al., 1986], [Brooke et al., 1988], [Dollfus and Suchail, 1988], [Kikuchi et al., 1988], [Lamy et al., 1988], [Le Borgne et al., 1988], [Metz and Haefner, 1988], [Sen et al., 1988], [Sen et al., 1989], [Sen et al., 1991a]). A detailed discussion showing how to separate these two components is given in ([Sen et al., 1989]).

In the late 19th century, photographic observations of many bright comets had helped to establish certain common properties of cometary polarization. The partial linear polarization has been found to depend on (i) the phase angle (angle between Sun-Comet-Earth), (ii) the wavelength of the observations, (iii) geometrical shape and size of dust particle and (iv) their composition. Dependence of polarization upon phase angle and wavelength has been obtained. Variations of polarization across distinct parts of a comet (coma, tail) as well as among different comets had been detected. All these polarization features had been attributed to the diffuse reflection and scattering of sunlight. They will be discussed in brief in the following sections and will be mainly aimed at the polarization which occurs due to the scattering of the sunlight by cometary dust particles. These studies help us in understanding different properties of cometary grains.

4.3 Phase-angle dependence of linear polarization

The phase angle dependence of the polarization is illustrated by the polarization phase curve (variation in polarization value of a body as a function of its phase angle). Because of inherent scattering-geometry and brightness limitations in ground-based comet observations, it is virtually impossible to determine the phase-angle dependence of polarization for a single comet in a large phase angle range 0°-130°. In practice, a composite phase-angle dependence of polarization is derived using observations of many comets. It can be done because P as a ratio does not need any normalization with distance and the polarization degree can immediately be used to derive polarimetric phase curves.

The light coming from a cometary atmosphere is a superposition of radiation scattered by dust particles and that emitted by the gaseous constituent. The scattering by dust and the resonance fluorescence from the most abundant cometary molecules CN, C_2, C_3, and NH_2 generally produce fundamentally different phase-angle dependencies of linear polarization. Since molecular, ionic, and atomic emissions contribute to all parts of the cometary spectrum, it is often difficult to identify the uncontaminated continuum and its intrinsic polarization. Solving this problem implies the need to perform spectropolarimetric observations with high spectral resolution or, at least, simultaneous polarimetric and spectrophotometric observations. [Mishchenko et al., 2010]

4.3.1 Important features of polarization:

Extensive polarimetric observations based on the use of filters separating continuum and molecular emissions have enabled astrophysicists to derive a composite phase-angle dependence of continuum polarization for the entire range of phase angles 0°-180° and identify a number of specific characteristics of cometary polarization. The similarities noticed between the phase curve of various objects include: (i) a negative branch for small phase angles, (ii) the inversion angle α_0 where the negative branch turns to positive, (iii) a positive branch for greater phase angles, with a maximum in the 90°-100° region, (iv) the values of maximum negative and positive polarization P_{max} and P_{min}, and (v) the phase angles where these are reached α_{max} and α_{min}, and the slope h of the curve at α_0. ([Zellner and Gradie, 1976], [Dollfus et al., 1988], [Levasseur-Regourd et al., 1990], [Mishchenko et al., 2010])

4.3.2 The two distinct branches:

Positive polarization branch (PPB): The linear polarization of light scattered by cometary dust is positive at phase angles $\alpha \geq 22°$ and negative at $\alpha \leq 22°$ for back-scattering geometries. In Fig. 4.1, the results of polarimetric observations of comets with the narrow-band filters BC and RC adopted for the International Halley Watch program (or with similar filters 5300/50 $\AA$, 4430/44 $\AA$, and 6420/26 $\AA$) have been shown. The errors in measurement are within the range 0.1%-1% depending on the brightness of a comet. The polarization values for different comets at similar phase angles are very similar, which testifies the similarity of the dust-particle morphologies. [Mishchenko et al., 2010]

Negative polarization branch (NPB): Observations of comet West revealed a negative branch of linear polarization at phase angles $\alpha \leq 22°$ [Kiselev and Chernova, 1978]. Subsequently, ([Kiselev et al., 2002], [Kiselev and Rosenbush, 2004]) observed similar phase-angle dependence of polarization for cometary

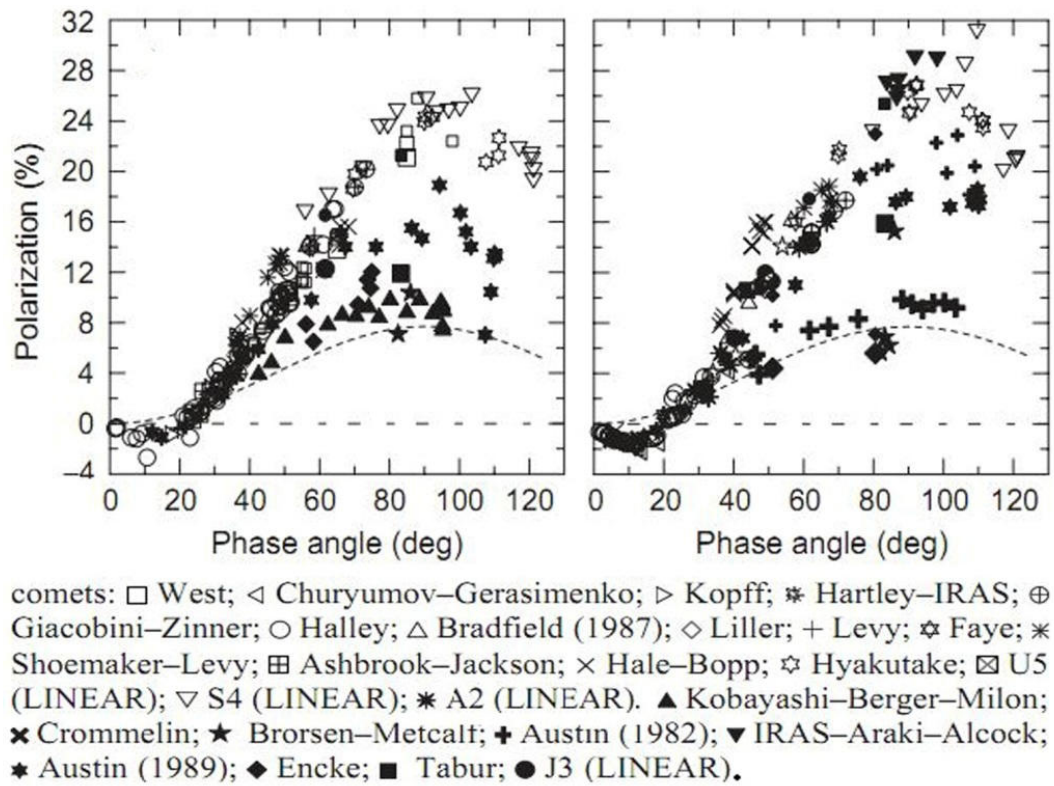

Figure 4.1: Positive polarization branch for several comets.
They are in the blue (left) and red (right) spectral continuum. Adopted from [Mishchenko et al., 2010].

grains and demonstrated this as inherent property of all comets. The justification of this empirical fact has been of utmost significance for the understanding of the properties of cometary dust as well as of the nature of light scattering by dust particles covering or forming various types of Solar System bodies. It is a common phenomenon for Solar System dust, where multiple scattering and interactions between the constituent grains inside aggregates play an important role.

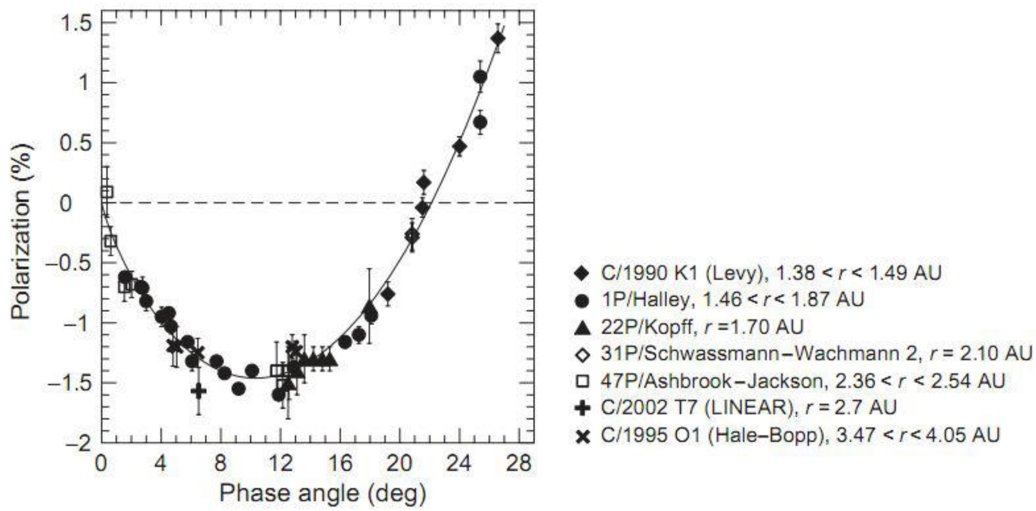

Figure 4.2: Negative polarization branch for several comets.
Adopted from [Mishchenko et al., 2010]

4.3.3 Model for polarization phase curve:

Öhman was the first to find that the degree of linear polarization changes with phase angle according to the following formula:

$$P(\alpha) = \frac{P_{90}\sin^2(\alpha)}{1 + P_{90}\cos^2(\alpha)} \tag{4.2}$$

where P_{90} is the maximal polarization at the phase angle α=90°. Öhman and many others ([Blackwell and Willstrop, 1957], [Bappu and Sinvhal, 1960]) modeled the phase-angle dependence of polarization in the continuum using the Eqn. (4.2), and found that it works well in the range α = 40°-80°. This relation has also been confirmed by numerous observations of molecular bands for many comets ([Blackwell and Willstrop, 1957], [Bappu et al., 1967], [Le Borgne et al., 1987], [Sen et al., 1991a]). The subsequent observations of some comets at large phase angles allowed to conclude that independently of the wavelength, the maximum of the cometary PPB occurs at max α = 95°; e.g. comets Hyakutake and S4 (LINEAR) [Kiselev and Velichko, 1998], comet IkeyaZhang [Velichko and Velichko, 2002].

[Lumme and Muinonen, 1993] suggested the following function as an empirical model for a polarization phase curve [Penttilä et al., 2005] -

$$P(\alpha) = b \sin^{c1}(\alpha) \cos^{c2}(\alpha/2) \sin(\alpha - \alpha_0) \tag{4.3}$$

The phase curve model in Eq. (4.2) has four parameters: b, α_0, c1 and c2. The parameter b (physically reasonable range is [0, 1]) is mainly connected to the amplitude of polarization. The parameter α_0 is the inversion angle. A physically reasonable range for α_0 is obviously [0°, 180°], although in observations the inversion angle seems to stay below $\sim$ 30°. The powers c1 and c2 have an influence on the shape of the phase curve. The parameter c1 mainly affects the position of the minimum and the second derivative of the curve, while c2 has influence on the maximum and on the asymmetry of the curve, moving the angle for maximum polarization away from 90°. These two parameters should have positive values. The collection of these four parameters offers a wide variety of different, realistic shapes for phase curves. The most important advantages are that, it can describe polarization throughout the phase angle range [0°, 180°]; the values of the function are limited to the range [-1, 1] (when the parameter ranges are correctly defined) and the important polarization feature, the inversion angle α_0, is explicitly included in the expression. This guarantees that the function is always physically reasonable. This function has been used by numerous authors to fit the observational data (e.g. [Goidet-Devel et al., 1995], [Levasseur-Regourd et al., 1996], [Hadamcik and Levasseur-Regourd, 2003b], [Hadamcik and Levasseur-Regourd, 2003c], [Hadamcik and Levasseur-Regourd, 2003a], [Kiselev et al., 2002]).

4.4 Classification of comets based on polarization

Comets are generally classified by their orbital properties into i) long period and ii) short period comets. They are considered to originate from two reservoirs: the Oort cloud and the Kuiper belt as discussed in chapter 1. There exist other ways of classification of comets. Among them, one is by their polarization properties and another is by their constituents (gas and dust).

Two classes of comets have been defined by their polarization values at large phase angles through relatively large apertures [Levasseur-Regourd et al., 1996]. From a data base of 22 comets and 750 points (mainly in the green and red spectral domains), Levasseur-Regourd with her colleagues pointed out a dichotomy between comets with respect to the maximum polarization (P_{max}) they attain for a phase angle α_{max} ($\approx 95 \pm 10°$). Some comets (e.g. West 1976 VI, P/Halley 1986 III, Bradfield 1987 XXIX, Levy 1990 XX) exhibit a rather large polarization maximum, with P_{max} about 25% and 30% respectively in the green and red domains. Other comets (e.g. Kobayashi-Berger-Milon 1975 IX and Austin 1990 V) exhibit a relatively lower polarization maximum, with P_{max} value about 10% and 15% for the same domains. These classes are called High-P_{max} comets and Low-P_{max} comets respectively. The negative branch through large apertures is somehow identical for all comets, except for observations of some comets in the near-infrared domain (e.g., comet Hale-Bopp, [Jones and Gehrz, 2000]; comet Schwassmann-Wachmann 3-C, [Jones et al., 2008]). It is therefore impossible to determine the class of comets with the low phase angle data base. A third class of comet has been mentioned by [Hadamcik and Levasseur-Regourd, 2003c]. The degree of polarization measured for comet HaleBopp at phase angles $34° - 49°$ is $\sim$4% higher than that for any other comet observed so far ([Kiselev and Velichko, 1997], [Hadamcik et al., 1997], [Hadamcik and Levasseur-Regourd, 2003b], [Hadamcik and Levasseur-Regourd, 2003c], [Jockers, 1997]). The negative branch is less deeper than that for other comets, mainly in the infrared (about zero at a wavelength of 2.2 μm for $\alpha \leq 20°$ [Jones and Gehrz, 2000].

The existence of these three polarimetric classes is most likely a clue to some significant differences in the bulk properties (albedo, size distribution, porosity) of dust in different comets. The phase angle at inversion (α_0) and the slope at

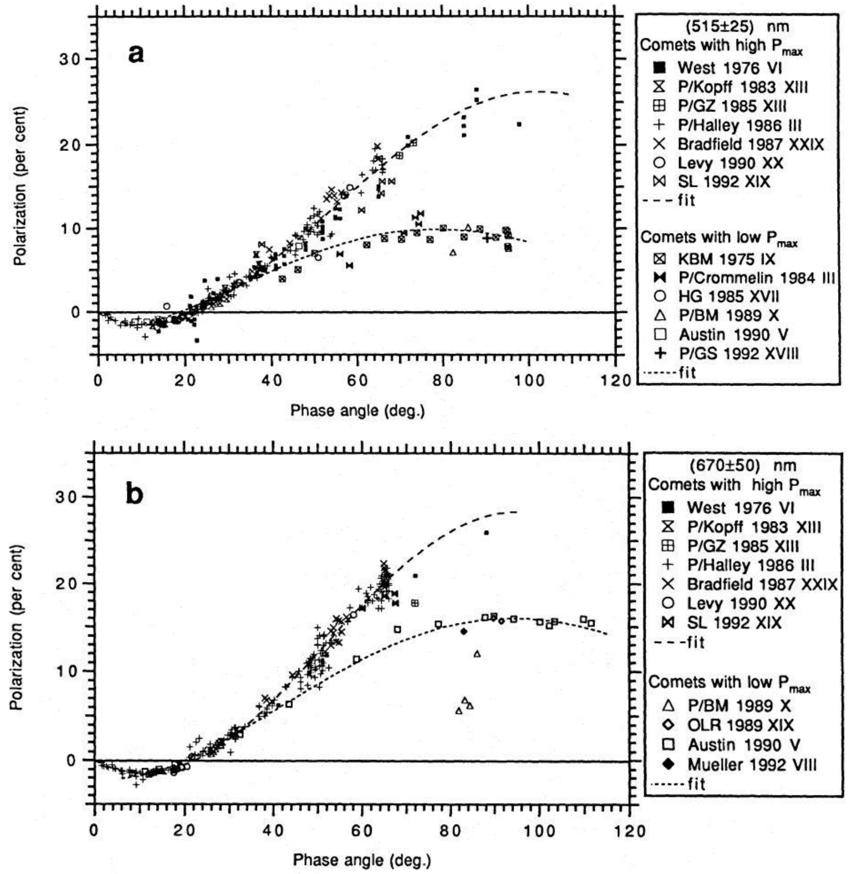

Figure 4.3: Evidence for two classes of comets from their polarimetric properties. *The polarization values are in green and red domain respectively in 'a' and 'b'. Dichotomy is noticeable above 35° phase angle. Adopted from [Levasseur-Regourd et al., 1996]*

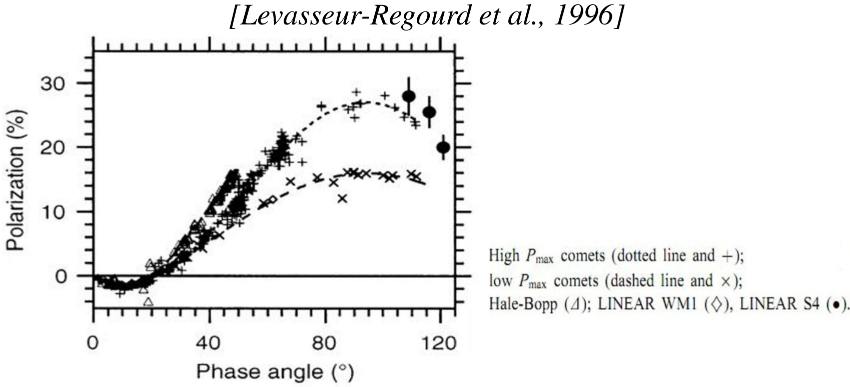

Figure 4.4: Showing third class of comets along with other two classes. *Adopted from [Hadamcik and Levasseur-Regourd, 2003c]*

inversion (h) seem to be slightly higher for comets belonging to first class than for comets belonging to the second class. A colour effect may be pointed out, the polarization slightly increases with increasing wavelength, from green to the red (and also to the near infrared) domains. Also, it may be noticed that the dispersion between the data obtained at various wavelengths is smaller for the comets with a large polarization at maximum than for the other ones.

Prior to the classification of comets based of its maximum polarization value, N. N. Kiselev [Dobrovolsky et al., 1986] had introduced another kind of classification of comets: (i) dust-rich comets exhibiting a strong continuum polarization, and (ii) gas-rich comets exhibiting a strong contribution from molecular emissions and a relatively weak contribution from continuum polarization. A correlation between the two ways of classification can be noticed as-

High-P_{max} and Dust-rich comets: An excellent correlation was found between comets of the high-P_{max} class and those with a strong 10 mm silicate features ([Kolokolova et al., 2004] and references therein). Their dust seems to be dominated by large aggregates of submicron-sized grains made of mixtures of silicates and carbonaceous compounds. These comets are often called dust rich. The fluffy particles can be easily accelerated by the gas flow [Köhler et al., 2007] and the jets extend over large distances.

Low-P_{max} and Gas-rich comets: The comets in the low-P_{max} class may be new comets without any jet structure or short-period comets with eventual dust concentration close to the nucleus. In visible wavelengths, the dust to gas ratio is generally low and the contribution of the gaseous species are more difficult to avoid. Some authors call this class 'gas rich' or 'dust-poor' comets ([Chernova et al., 1993] [Kiselev and Rosenbush, 2004]). The classification by the value of the linear polarization is correct for observations through large apertures; it is correlated to the absence or faintness of infrared silicates emissions corresponding to more compact particles ([Kolokolova et al., 2004], [Kolokolova et al., 2007]). The physical properties of the particles are easier to be deduced by considering images than only large apertures data. For example, imaging techniques reveal high inner coma polarization [Jockers et al., 2005] for some low-P_{max} comets. The concentration of large compact particles may be higher at relatively small distances from the nucleus and as deduced from laboratory experiments, large dark compact particles present very high polarization values. However, work by [Das et al., 2004], showed that the polarimetric data of all the comets can be explained by a smooth varying particle size distribution, where the dynamically older comets contain larger sizes of dust grains.

4.5 Morphological features

Many comets exhibit detailed, well-defined features in their comae. Some prominent types of features include jets (radial structures produced by isolated active regions, or sources, that emit collimated streams of gas and dust), fans (jet-like structures that tend to be broader and more diffuse than jets), spirals and arcs (outflowing material from jets on a rotating nucleus that form archimedean spirals, or partial segments of spirals, respectively), and coma asymmetries (some regions of the coma appear brighter than others). The study of these features provides explanation for the coma morphology. Their (features) presence indicates that the surfaces of the nuclei of these comets emit materials anisotropically. The existence of isolated source regions also provides a natural explanation for a variety of other phenomena observed in comets, including seasonal variations in the production rates, nongravitational accelerations of the comets orbit, and changes in the rotation state of the nucleus. [Schleicher and Farnham, 2004]

Various techniques are used to understand the role that the active regions play in the comet's behavior. Some of the properties are determined through coma modeling, some could be found using other techniques like light-curve variations measurement, many could otherwise only be found via spacecraft encounters. The majority of the analyses of comet's coma features are performed using images obtained with broadband and narrowband continuum filters. The technique is useful because the dust coma tends to show clearer, more well-defined structures than the gas species. However, gas and ions have their own contributions which tend to be overwhelmed by the dust features. The use of narrowband filters helps to isolate the gas features. The little gas contamination can be removed from images obtained with narrowband continuum filters to leave the pure dust coma. Similarly, with careful calibration the underlying continuum can be removed, leaving images of the pure gas coma ([Schulz et al., 1993], [Schulz et al., 2000], [Farn-

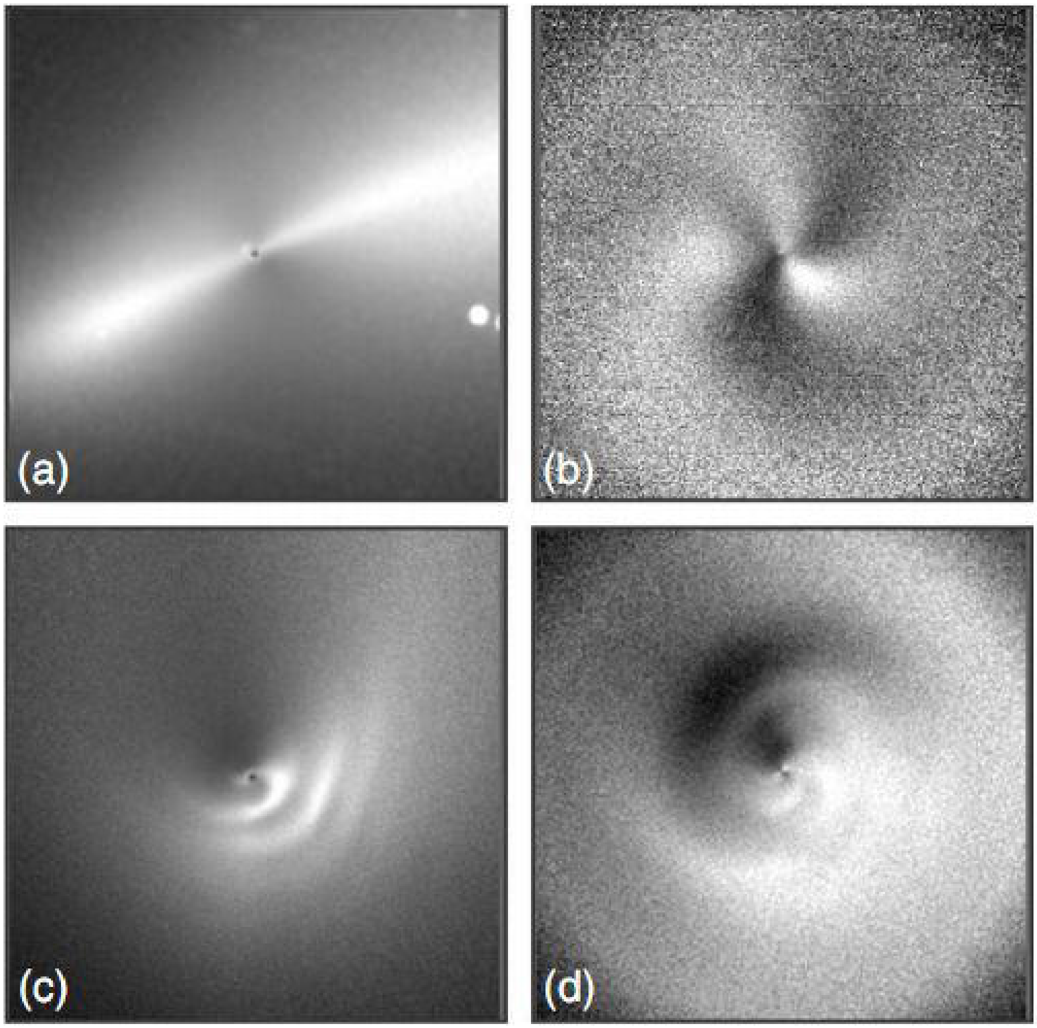

Figure 4.5: Different radial and azimuthal structures showing coma morphology. *Adopted from [Schleicher and Farnham, 2004]*

ham et al., 2000]). The pure gas images can then be enhanced or modeled, in the same manner as the dust images, to learn about the gas properties and to provide additional constraints on the nucleus properties.

Many features are overwhelmed by the bulk radial brightness fall-off of the coma and only become obvious when the image has been processed in some manner (image enhancement techniques). Unfortunately, enhancing an image, by definition, alters the image, and not always in the manner that is expected or desired. Thus, any processing technique should be used with caution. Potential dangers include introducing artifacts that can be misinterpreted as real structures or shifting the apparent positions of features. A number of basic processing methods are discussed in ([Schwarz et al., 1989], [Larson and Slaughter, 1991], and [Farnham and Meech, 1994]) - (a) 1/ ρ profile, divided out, (b) 1/ ρ profile, subtracted out, (c) Azimuthal-averaged profile divided out, (d) Linear shift difference in both the vertical and horizontal directions, (e) Rotational shift difference, (f) Laplace filter, (g) Unsharp mask with a three-pixel Gaussian smoothing kernel, (h) Radial gradient filter, (i) Azimuthal renormalization. Among them, rotational gradient method introduced by [Larson and Sekanina, 1984] is one of the important and useful methods, which has been applied in the present study.

For high gas-to-dust comets, direct measurements of the nucleus [Lamy et al., 2004] are more efficient with narrowband filters than broadband ones, because continuum filters exclude the gas contribution and make the nucleus stand out more against the coma. In plasma tail studies, the narrow passbands will isolate CO^+ or H_2O^+ much more efficiently than broadband filters, increasing the contrast of the plasma features against the background. Furthermore, with proper calibration, the continuum can be removed from the ion images to reveal the features very close to the nucleus. Dust, gas, and ion features have been observed and studied in many comets, with recent examples including Halley, Hyakutake, Hale-Bopp, and Borrelly. Although the detailed morphology in each comet is unique, the features can generally be classified into two main categories: azimuthal and radial (or a combination of the two). [Schleicher and Farnham, 2004]

Because most of the materials from a jet expand radially away from the surface, the appearance of structures in the coma is strongly dependent on the geometric viewing conditions and the rotation state of the nucleus. Radial features are produced when the jet is on a slowly rotating nucleus or if the active region is near the rotation pole, as is the case for Comet 19P/Borrelly ([Samarasinha and Mueller, 2002], [Farnham and Cochran, 2002], [Schleicher et al., 2003]). Solar radiation pressure can act on the dust grains to produce envelopes that can be mistaken for arcs, while anti-tails and neck-line structures can mimic radial structures [Fulle, 2004]. However, both of these cases are only observed in continuum images and involve relatively unique circumstances and geometric alignments, which can be investigated to avoid misinterpretation of the results.

4.6 Imaging polarimetry

It is a technique where images of comet at various polarization modes are combined to obtain a final polarization image of the comet, which displays distribution of degree of polarization in different parts of comet and allows to study the variation. The images (presently obtained using CCD) of intensity and polarization of comets can help to find out a correlation between the occurrence of different structures (mentioned in section 4.5) and corresponding variation in polarization values with the surrounding coma.

Most of the observations are taken through apertures, rather than imaging. Comet P/Halley was imaged polarimetrically, for the first time, in the coma and tail region on 5th January 1986 at 15:55 UT by [Sen et al., 1990] and at 16:50 UT by [Eaton et al., 1988]. In the inner coma, [Sen et al., 1990] noticed a small region with very low ($<2\%$) polarization . But in the tailward direction beyond the outer coma two separate regions of enhanced polarizations ($>8\%$) are found. [Eaton et al., 1988] observed a similar region of high polarization, but at a much closer distance to the nucleus. These regions are probably connected with jet ativities in the comet. The low polarization region in the inner coma can also be connected with a fresh dust jet ejecta, where the low polarization is resulting from multiple scattering in a region of high dust concentration, in the fresh ejecta.

The observed variation in polarization values in different region as explained by [Eaton et al., 1988] and [Sen et al., 1990], can be due to several mechanisms. The polarization values depend upon- size distribution of the grains which could be different along observed structures from the surrounding coma; also the material of the grains could have a different refractive index and the ratio of dust to gas emission could be different in different regions (coma, jets). High polarization region might have high concentration of smaller size particles. Grains, after they are released from the nucleus, may change their optical properties (like refractive indices) with time, due to evaporation of volatiles. Also grains which are originally released from the nucleus, will break up into smaller pieces as they move along the tail. Again the observed polarization has contribution from the cometary molecular emission. A reduction in gas to dust ratio can also increase the observed polarization in a particular region. Also when a dust jet is ejected from the nucleus, the smaller-size particles travel further, away from the nucleus compared to the large size particles, owing to their stronger coupling with the gas outflow and also due to more effective radiation pressure.

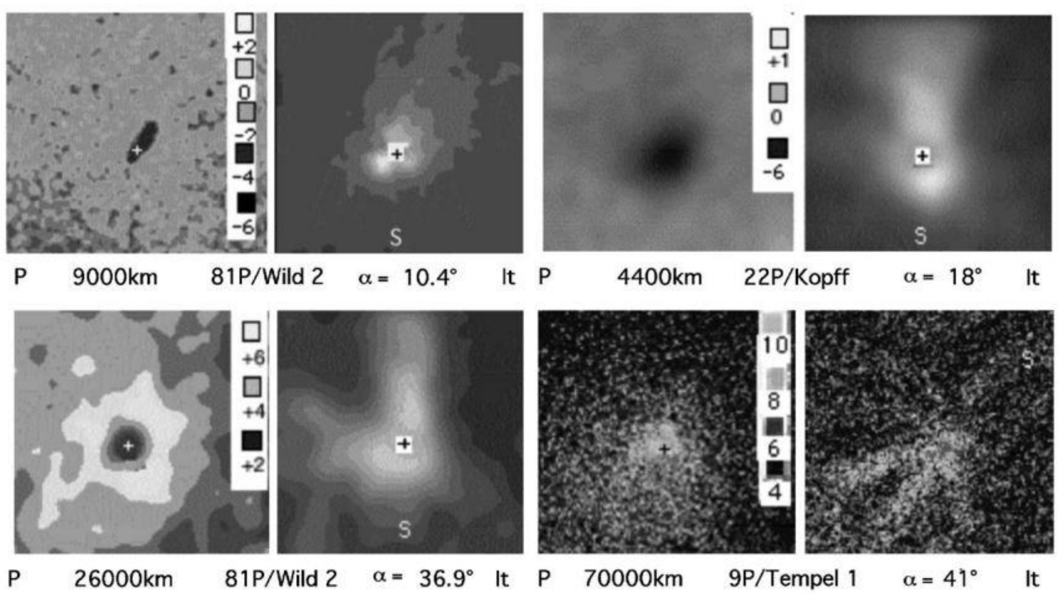

Figure 4.6: Polarization maps and emphasized intensity images by a rotational gradient method emphasizing the jets and fans regions.
Red filters (650 nm, $\Delta\lambda$50 nm). S is solar direction. Field of view indicated under each polarization map (km). P and It indicates polarization and intensity image respectively. Adopted from [Hadamcik and Levasseur-Regourd, 2009]

Several other authors have reported imaging polarimetry results later. In the following paragraphs, polarization map of some comets by other authors will be discussed to give an impression on spatial variation of polarization.

Comet 22P/Kopff: The polarimetric observations of comet 22P/Kopff [Hadamcik and Levasseur-Regourd, 2003c] were made at 18° phase angle. Around the optocenter (optical center or photocenter), the negative polarization region diameter was about 1500 km and P increased slightly, from 6% up to 1%, with increasing nucleus distance (Fig. 4.6). The tailward structure has no counterpart on the polarization map, indicating no difference between the dust properties.

Comet 81P/Wild 2: [Hadamcik and Levasseur-Regourd, 2003c] observed comet 81P/Wild 2 at phase angles about 10° and about 36°). At small phase angles the polarization was strongly negative (-5%) in the inner coma (1000 km) and increased up to about -2% in an aperture of 9000 km. Dust jets were detected on the emphasized intensity image but they have no obvious counterparts on the polarization map (Fig. 4.6). At intermediate phase angles (about 36°), the polarization value close to the nucleus was smaller than in the surrounding and increased with increasing aperture. On the polarization map, a higher polarization region was detected, corresponding to the faint structures on the emphasized intensity image (Fig. 4.6).

Comets 10P/Tempel 2, 19P/Borelly: Observing comet 10P/Tempel 2 (α=42.4° and 32.2°) and comet 19P/Borelly (α=35°) in the near-infrared K-band, [Kelley et al., 2004] found no difference between the polarization of the jets and the other coma regions, suggesting similar properties for the particles located in the jets and in the surrounding coma. Observed in the K-band, comet 19P/Borelly seems to belong to the high-P_{max} class and 10P/Tempel 2 to the lower polarization class.

Comet 9P/Tempel 1: [Hadamcik et al., 2007a] reported evolution of the polarization in the coma by polarimetric imaging, before and after the collision of Deep Impact (DI). Before impact (α=41°), polarization measurements were done to study the quiet coma and it was below the high-P_{max} comets synthetic phase curve ([Kiselev et al., 2008], [Hadamcik et al., 2007a]). The higher polarization region around the nucleus (about 1600 km radius) is probably due to relatively compact large slowly moving particles, which were mainly found close to the nucleus. The high polarization value indicates their important absorption (interpretation by experimental simulations; [Hadamcik et al., 2009]). Such particles were observed before impact by in situ measurements; [Farnham et al., 2007] suggested a speed of about 12m/s. After impact a large polarization in the central part of the coma was also found; but the 'quiet' coma ejection of particles and jets did not change after the impact. Besides, a large amount of high-speed dust was ejected during the collision in a structure called 'plume'. Its polarization was high. This high polarization is probably due to the presence of fluffy aggregates made of submicron to micron-sized grains, as corroborated by the results of other observational techniques such as infrared spectroscopy.

Split comet 73P/Schwassmann-Wachmann 3: The two largest fragments B and C of comet 73P/S-W 3 were observed by different teams. ([Hadamcik et al., 2007a], [Bonev et al., 2008], [Jones et al., 2008], [Ho et al., 2008]) have detected sub-fragments and/or clusters of sub-fragments on fragment B images (before outburst of fragment B on May 3). The sub-fragments outflow hit the outflow of particles pushed in the tail direction and changed the intensity gradients and the polarization values. [Jones et al., 2008] found a lower polarization around the main nucleus of fragment C and an increase of polarization with nucleus distance attributed to fragmentation of the particles or to evaporation of volatiles. [Hadamcik et al., 2007a] found an significant evolution of the polarization values and of the structures shape in the near nucleus region, probably related to the nucleus rotation with a higher and lower polarization region changing with time and location in the coma. The observations through red and near-infrared I and H filters, up to about a 60° phase angle showed that the data points were close to the high-P_{max} comets synthetic phase curve for the two fragments. At larger phase angles, all the data points (for B and C) followed the same trend and were below the synthetic red curve.

Comet 67P/Churyumov-Gerasimenko: [Hadamcik et al., 2010] studied the comet polarimetrically and reported that, sixty days before perihelion (α=36°), the polarization map is quite uniform in a field of view of 12000 km diameter, without any feature, indicating that there is no major difference in the physical properties of the dust between the tailward structure and the other parts of the coma, including the region surrounding the photocenter. Three weeks after perihelion (α=29°), the polarization close to the optocenter is about 6%. The polarization in the jet features is (4-6)% for a surrounding polarization of (2-3)%. The jet features are mainly found in the south and sunward directions, with a bit in the tailward direction. The higher polarization regions are correlated to the features observed on the rotational gradient intensity images. The polarization maps are different in March as compared to December, indicating dusts with physical properties closer to those usually observed for active comets.

103P/Hartley 2: Polarization maps retrieved for two epochs at α=46.8° and 58.8° have been reported by [Hadamcik et al., 2013]. Features close to the optocenter with a higher polarization (decreases further away) are observed on all the maps for the red filters. The solar-antisolar asymmetry observed tailward in intensity is also observed in the polarization maps; however, the highest polarization region corresponds to sunward jets. The jets locations are similar to the ones in the intensity images (treated by the rotational gradient method). Their extension changes with time and the dust seems to be sensitive to radiation pressure, and pushed tailward, indicating dust with higher β ratio (ratio between solar radiation pressure force and solar gravity), i.e. rather micron-sized and/or low density (typically fluffy) dust.

4.7 Numerical simulation

Numerical simulation of polarization by scattering of electromagnetic waves and other grain properties allows us to match the simulated results with observed results and understand the cometary phenomenon better. Gustov Mie [Mie, 1908] proposed a theory of scattering by a homogeneous, isotropic and smooth sphere of arbitrary size and refractive index. Many authors ([Kiselev and Chernova, 1979], [Kiselev and Chernova, 1981], [Myers and Nordsieck, 1984], [Brooke, 1987], [Sen et al., 1991b], [Das et al., 2004]) have reported their works on cometary polarization using Mie-theory. Based on the power law distribution [Mazets et al., 1986] and Mie Scattering codes; [Mukai et al., 1987] and [Sen et al., 1991b] analyzed the polarization data of comet Halley and derived a set of values of complex refractive index that characterizes the composition of cometary grains. [Sen et al., 1991b], using Mie scattering codes, analysed the polarimetric observation of comet Austin. They found differences in phase angle dependence at the same wavelength for these two comets (Halley and Austin). It was argued that observed differences can be explained if either size distribution or composition is different for the comets. Using the same scattering codes, [Das et al., 2004] concluded that the grains which are processed more by solar radiation do contain a relatively smaller number of finer grains. From that work, they found grains of comet Levy 1990XX are much smaller than that of Hyakutake, Austin, Bradfield, Hale-Bopp and Halley.

But it is now well accepted that cometary grains are not perfectly spherical. These are fluffy or porous aggregates with irregular or spheroidal shape ([Greenberg and Hage, 1990], [Kimura, 2001], [Kimura et al., 2006]). Several methods have been developed to compute light scattering by non-spherical particles. The more natural grain shape is not only non-spherical, but also they are of some complex geometry. The individual grains are compilation of many spherical and non-spherical grains. The above technique cannot be used for such complex geometries. To simulate natural aggregates, several investigators ([Kimura et al., 2003], [Kimura and Mann, 2004], [Kimura et al., 2006], [Kolokolova et al., 2007], [Das et al., 2008b], [Das et al., 2008b]) built aggregates using ballistic aggregation procedure ([Meakin, 1983], [Meakin, 1984]). In the case when the procedure allows only single particle to join cluster of particles, the aggregate is called Ballistic Particle Cluster Aggregate (BPCA). If the procedure allows cluster of particles to stick together, the aggregate is called ballistic cluster cluster aggregate (BCCA). Two other types of aggregation are: Ballistic Agglomeration with one Migration (BAM1) and Ballistic Agglomeration with two Migrations (BAM2). The newly introduced BAM1 and BAM2 clusters have geometries that are random but substantially less fluffy than BPCA, BCCA clusters. The irregular grain characteristics of comets are mostly studied by T-matrix theory [Watermann, 1965], Discrete Dipole Approximation (DDA) ([Draine, 1988], [Draine and Flatau, 2013]).

Using T-matrix theory and considering the grains to be of prolate shape (aspect ratio 0.48), [Das and Sen, 2006] reported their work on polarization of comet Levy 1990XX. The fitting by this model was more close to the observed polarization data as compared to the model with ideal Mie spheres. The fitting included the observed negative branch of polarization also and they concluded that compact prolate grains can explain observed polarization better than spheres. But the prolate grain model could not produce better fit for comet 1P/Halley and C1995/O1 Hale-Bopp. This itself showed the failure of spheroidal model for cometary grains.

[Das et al., 2008b], performed calculations on scattering properties of comet Levy 1990XX by superposition T-matrix method [Mackowski and Mishchenko, 1996] using BPCA or aggregates, taking upto 128 spherical monomers (N) of different compositions of silicates & carbonaceous compounds. To simulate observed polarization data, the complex refractive index (n,k) was used as free parameters. They found that the silicate compositions can explain the observed data better. [Das et al., 2008a] reported simulated polarization curve of comet Hale-Bopp at λ=0.485 μm & λ=0.684 μm. They concluded that the difference in polarization of comet Levy 1990XX & Hale-Bopp is due to the change in refractive index of the dust grains, however size parameter remained fixed. [Das et al., 2010] and [Paul et al., 2010] reported the polarization data of comets C/1996 B2 Hyakutake & C/2001 Q4 NEAT respectively using same technique at several wavelengths. Here monomer radius was varied with different wavelengths, but the size parameter remained almost the same.

STARDUST space mission on comet 81P/Wild2 has suggested the cometary grains to be mixture of both compacts and aggregates. ([Lasue et al., 2009], [Kolokolova and Kimura, 2010b], [Das and Sen, 2011]) have reported their works considering such model i.e. mixture containing both compact and aggregate particles. [Das et al., 2011], simulated the observed polarization data of comet 1P/Halley taking a mixture of prolate, spherical and oblate compact particles and using BCCA & BAM2 aggregates, with a suitable mixing ratio as 13:7. With the power law size distribution $n(a) \sim a^{-2.6}$, the best fitted theoretical polarization vs phase curves produced using Superposition T-matrix code at four wavelengths, viz. 0.365 μm, 0.485 μm, 0.670 μm, 0.684 μm were reported. They found the silicate compositions to dominate over organic refractory in 1P/Halley.

4.8 Importance of polarimetric study

Polarimetric study is a diagnostic tool to investigate the physical properties of the particles. The observed phase-angle and wavelength dependence of polarization as well as its spatial and temporal variations depend on the specific processes of light scattering, the microphysical parameters of the constituent dust particles, the distribution of dust and gas in the coma, and possible alignment of nonspherical dust grains. This makes polarimetry an essential tool for the determination of optical and microphysical properties (size, refractive index, morphology etc) of cometary dust particles. Another important function of polarimetric observations is to facilitate taxonomic classification of comets and to help relate the properties of cometary dust to the origin and evolution of a comet and also solar system.